American Journal of Water Science and Engineering
2021; 7(3): 103-112
http://www.sciencepublishinggroup.com/j/ajwse
doi: 10.11648/j.ajwse.20210703.12
ISSN: 2575-1867 (Print); ISSN: 2575-1875 (Online)

Forecasting of Monthly Flow for the White Nile River (South Sudan)

Tariq Mahgoub Mohamed

Department of Civil Engineering, Elnasr Technical College, Omdurman, Sudan

Email address:
tariqcivil73@yahoo.com

To cite this article:
Tariq Mahgoub Mohamed. Forecasting of Monthly Flow for the White Nile River (South Sudan). *American Journal of Water Science and Engineering.* Vol. 7, No. 3, 2021, pp. 103-112. doi: 10.11648/j.ajwse.20210703.12

Received: March 31, 2021; **Accepted**: April 22, 2021; **Published**: August 18, 2021

Abstract: Forecasting of monthly streamflow for the White Nile River at Malakal station is a crucial aspect for different water resources projects in both countries Sudan and South Sudan. For instance, the operation of Jabal al Awliya dam in central Sudan entirely depends upon the measured flow of this station. In this paper, linear stochastic models well-known as seasonal autoregressive integrated moving average [SARIMA] models were used to model and forecast monthly flow of White Nile River in Malakal station, South Sudan. For the analysis, monthly flow data for the years running from 1970 up to 2013 were used. A scrutiny of the original series proves a yearly seasonal pattern. The results of Phillips-Perron (PP) test and Augmented Dickey Fuller (ADF) test on the streamflow series show that this series is not stationary. This non-stationarity was removed using first order seasonal differencing (i.e. twelve-monthly) preceding to the development of the model. The SARIMA $(1,0,1)\times(0,1,1)_{12}$ model was selected as the most suitable for modeling and forecasting monthly flow for White Nile River. It was found that the model was proper to forecast three successive years of monthly flow, which may help the experts to institute priorities for various water resources management in both countries.

Keywords: White Nile River, South Sudan, Malakal, Stochastic Models, SARIMA

1. Introduction

The Nile River is the longest river in the earth planet, nearly 6700 km long, with total catchment area of about 3.2 million km^2. The Nile water is shared between eleven riparian countries which together populate more than 487 million peoples [1]. There are three major tributaries to the Nile River, which are the Blue Nile, the White Nile, and the Atbara River. The entire flow of the Nile River is about 84.1 billion m^3 at Aswan dam, Egypt. The Blue Nile and the Atbara River contributes about 61 billion m^3, or 72% of the overall flow. The remaining 28% is derived from the White Nile River. The contribution of White Nile is very essential as it gives a continuous flow throughout the year [2]. The White Nile originates from the Equatorial Lakes region in central part of Africa. Its sub basin involves catchment areas in Burundi, Kenya, Republic of Congo, Republic of Sudan, Rwanda, South Sudan, and Uganda. The White Nile enters South Sudan at Nimule city and goes through Juba city, the capital, to spread out in large swamps called the Sudd region. The swamps are considered as one of the largest wetland areas in the world, covering an area of more than 30000 km^2. At this area, the White Nile branches into many smaller rivers and is fed afterward by Bahr el Ghazal River. A large amount of the White Nile water evaporates in the swamps area. The Jonglei canal project plans to shorten and direct the flow of the water through the Sudd areas. When completed, the canal is designed to divert about 20 million m^3 of water per day past the swamps, which will save about 4.7 billion m^3 per year of water evaporation in the swamps [3].

At Malakal city, the capital of Upper Nile State, the White Nile is merged by its last tributary, the Sobat River. The section of the White Nile River situated between Nimule and Malakal is named as Bahr el-Jebel. Then the White Nile continues north to Khartoum city crossing the Jabal al Awliya dam. The dam was built in 1937 to control the level of the Nile River downstream. It is one of the largest reservoirs in Sudan. Jabal al Awliya dam serves the irrigation needs of many projects in central Sudan. The White Nile joins the Blue Nile at Khartoum city to form the Nile River. Later, River Atbara, which is the last stream flowing into the Nile River, enters the Nile at Atbara city nearly 320 km north of Khartoum. Finally, the Nile travels north through the Nubian Desert and Egypt to reach its last destination in the

Mediterranean Sea.

Time series forecasting of hydrologic variables, such as streamflow, is an important phase in analysis and planning of different water resources systems. For instance, monthly streamflow forecasting is useful in reservoir operations, irrigation management and different aspects of water resources management and planning.

Forecasting streamflow values accurately is significant for different water resources studies [4, 5]. Short-term flow forecasting is essential for flood protection works; medium-term forecasting is useful for reservoir operation; long-term forecasting is valuable for water resources management and planning [6-11]. During the last decades, a large number of forecasting models have been used for streamflow forecasting such as rainfall-runoff models, low flow recession models, regression models, time series models and artificial neural network models [6, 12, 13]. The time series models, including the autoregressive integrated moving average (ARIMA) models and seasonal autoregressive integrated moving average (SARIMA) models, have been widely used in streamflow forecasting [14-21]. Rabenja et al. [18] forecasted both monthly rainfall and the discharge of the Namorona River in Madagascar using ARIMA and SARIMA models; they concluded that the SARIMA model is the more adapted for the forecasting of the data of the rainfall and the monthly discharge. Valipour [19] modeled the long-term runoff in the United States adopting the stochastic SARIMA and ARIMA models. He found that the accuracy of the SARIMA model is better than that of the ARIMA model.

This study applied the seasonal autoregressive integrated moving average (SARIMA) models to monthly streamflow forecasting for the White Nile River at Malakal station, South Sudan.

2. Materials and Methods

2.1. Site Description

The White Nile River has been measured at Malakal, South Sudan, since the year 1905. Malakal city lies on the eastern bank of the White Nile, just downstream of its meeting with the Sobat River. The city is located in the northeast part of South Sudan, near to the borders with the Republic of Sudan.

Malakal station is situated at 9.33° N latitude and 31.39° E longitude with altitude 387 meters above sea level, Figure 1. The averages of annual rainfall and temperature for the region are 782 mm and 28.1°C respectively. In addition, the annual average number of rainy days is 175 days and the average annual potential evapotranspiration is nearly 2021 mm [22].

Malakal station represents the contribution of White Nile, Sobat River, and Bahr el Ghazal basin. The flows measurements at Malakal are precise because the numbers of gauging have been sufficient and the rating curve is very good [23].

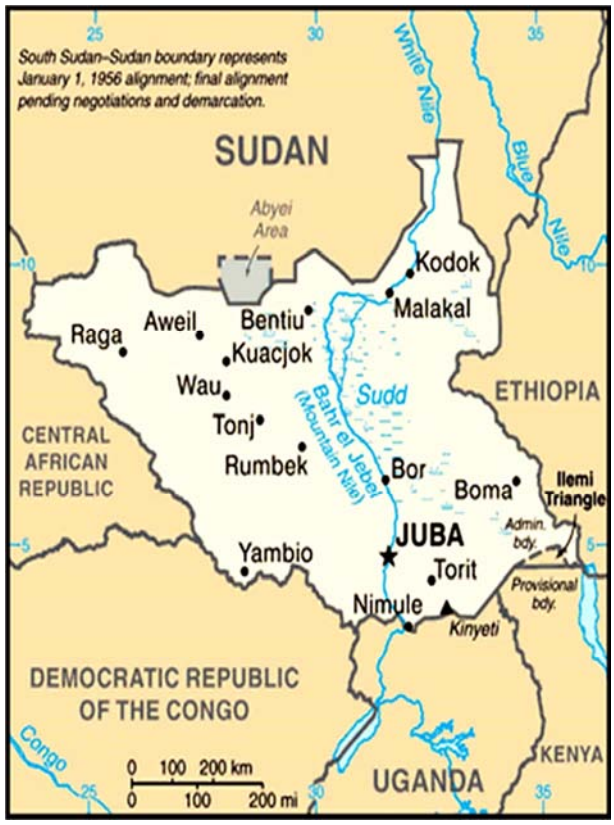

Figure 1. *Malakal city on the White Nile River – South Sudan.*

Source: (http://aemstatic-ww1.azureedge.net/content/dam/hydroworld/online-articles/2015/April/South%20Sudan.gif)

2.2. Data

Streamflow forecasting is crucial aspect for water resources management and flood protection. Monthly streamflow forecasting is helpful for reservoir operation. For example, the operation of Jabal al Awliya dam in central Sudan is entirely depending on the measured flow of Malakal station.

Daily and mean monthly streamflow data for the White Nile River at Malakal gauging station, South Sudan, were obtained from the Ministry of Water Resources and Electricity, covering the period 1970–2013. The mean monthly data is presented graphically in Figure 2.

According to the records, from 1970 to 2013, the highest amount of flow at Malakal was 131.74 M m^3/day recorded in November 1970; and the lowest amount of flow was recorded in April 2010 at 45.35 M m^3/day. The average daily annual flow for the river is 84.68 M m^3/day.

The number of observations for the specification of the SARIMA models must be at least 50 and preferably 100 for efficient estimation [24]. For the model selection, the chosen part of the data is ranged from January 2000 to December 2010 and the remaining data from 2011 to 2013 was considered in forecasting estimations of the model.

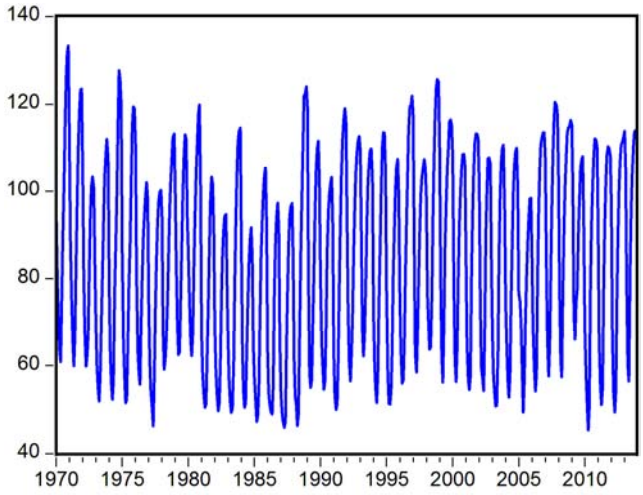

Figure 2. *Mean monthly flow data for White Nile River at Malakal station [1970-2013] in M m^3 per month.*

2.3. Modeling by SARIMA Methods

A time series is said to be stationary if it has constant mean and variance. A stationary time series can be modeled in numerous ways: an autoregressive (AR) process, a moving average (MA) process, or an autoregressive and moving average (ARMA) process. Although, an ARMA model deal with stationary data, ARMA models can be applied to non-stationary series by permitting differencing of data series. These models are called autoregressive integrated moving average (ARIMA) models. A time series may have non-seasonal and seasonal characteristics.

2.3.1. Non-seasonal ARIMA Model

The general structure of non-seasonal ARIMA model is AR to order p and MA to order q and operates on dth difference of the time series X_t; therefore a model of the ARIMA family is classified by three parameters (p, d, q) that can have zero or positive integral values. The general non-seasonal ARIMA model may be written as

$$\phi(B)\nabla^d X_t = \theta(B)\varepsilon_t \quad (1)$$

Where $\phi(B)$ and $\theta(B)$ are polynomials of order p and q, respectively. B is the backshift operator defined as $B^m X_t = X_{t-m}$, ∇ is the difference operator ($\nabla = 1 - B$) and ε_t is assumed to be a Gaussian white noise process with mean zero and variance σ^2.

$$\phi(B) = (1 - \phi_1 B - \phi_2 B^2 - \cdots \phi_P B^p) \quad (2)$$

and

$$\theta(B) = \left(1 - \theta_1 B - \theta_2 B^2 - \cdots \theta_q B^q\right) \quad (3)$$

2.3.2. Seasonal ARIMA Model

Frequently time series have a seasonal part that repeats every s observations. For monthly observations s=12 (12 in 1 year), for quarterly observations s=4 (4 in 1 year). Box et al. [24] has generalized the ARIMA model to deal with seasonality, and define a general multiplicative seasonal ARIMA model, which are generally known as SARIMA models. In short form the SARIMA model expressed as ARIMA (p, d, q) x (P, D, Q) s, which is written as

$$\phi_p(B)\Phi_p(B^s)\nabla^d\nabla_s^D(X_t) = \theta_q(B)\Theta_Q(B^s)\varepsilon_t \quad (4)$$

Where p is the order of non-seasonal autoregression, d the number of regular differencing, q the order of non-seasonal MA, P the order of seasonal autoregression, D the number of seasonal differencing, Q the order of seasonal MA, s is the length of season, Φ_p and Θ_Q are the seasonal polynomials of order P and Q, respectively.

SARIMA models development consists of the next three stages: model identification, parameters estimation and diagnostic checking. At the first stage, a preliminary SARIMA model is proposed from the analysis of the sample autocorrelation function (ACF) and partial autocorrelation function (PACF), allowing us to determine the parameters d, D, p, q, P and Q. The model that gives the minimum Akaike Information Criterion (AIC) [25] and Hannan-Quinn Criterion (HQ) is chosen as best model [26, 27]. After that, the non-seasonal and seasonal AR and MA parameters are estimated at the second stage. Finally, the diagnostic checking stage verifies whether the suggested model is adequate or not. If the model is considered adequate, it can be applied for forecasting future values; if not; the procedure is repeated until an adequate model is found. The flow chart of SARIMA model was drawn in Figure 3.

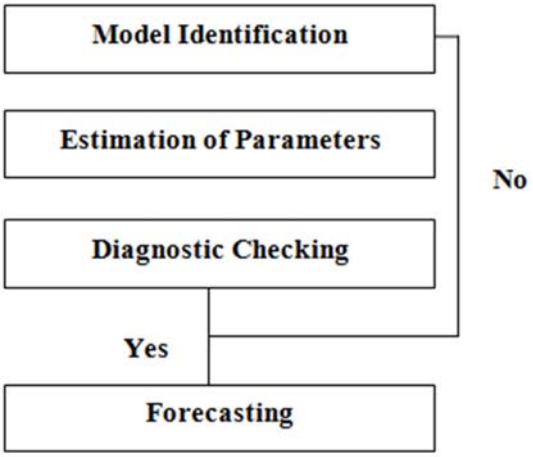

Figure 3. *Flow chart of SARIMA model.*

2.4. Tests of Stationarity

The first part in the identification phase is to examine the stationarity of the time series. This is done with the Augmented Dickey-Fuller (ADF) test and the Phillips-Perron (PP) test as explained in this section. There are other tests like the Kwiatkowski-Phillips-Schmidt-Shin test [28] and Zivot and Andrews test [29].

2.4.1. The Augmented Dickey-Fuller (ADF) Test

The Dickey-Fuller (DF) test is one of the most popular tests for unit root. The model is written as:

$$\Delta y_t = \alpha y_{t-1} + \dot{x_t}\delta + \epsilon_t \quad (5)$$

Where $\dot{x}_t$ are optional exogenous regressors which may consist of constant, or a constant and trend, α and δ are parameters to be estimated, and the ϵ_t are assumed to be white noise [30].

The model described above is valid only if the series is an AR (1) process. If the series is correlated at higher order lags, the assumption of white noise disturbances ϵ_t is violated. When a series is correlated at higher lags, the appropriate test is the Augmented Dickey-Fuller (ADF) which controls for higher-order correlation. The ADF test it is based on the following model

$$\Delta y_t = \alpha + \beta t + (\rho - 1)y_{t-1} + \delta_1 \Delta y_{t-1} + \cdots + \delta_{p-1}\Delta y_{t-p+1} + \epsilon_t \quad (6)$$

Where α is a constant, β the coefficient of a simple time trend, ρ is the parameter of interest, Δ is the first difference operator, δ_i are parameters and p the lag order of the autoregressive process.

2.4.2. The Phillips-Perron (PP) Test

Phillips et al. [31] develop an alternative nonparametric method for checking stationarity. The PP method estimates the DF test equation , and modifies the *t*-ratio of the α coefficient so that serial correlation does not affect the asymptotic distribution of the test statistic [30]. The test is based on the statistic:

$$\tilde{t}_\alpha = t_\alpha \left(\frac{\gamma_0}{f_0}\right)^{1/2} - \frac{T(f_0 - \gamma_0)(se(\hat{\alpha}))}{2 f_0^{1/2} s} \quad (7)$$

Where $\hat{\alpha}$ is the estimate, and t_α the *t*-ratio of $\alpha, se(\hat{\alpha})$ is coefficient standard error, and *s* is the standard error of the test regression. In addition, γ_0 is a consistent estimate of the error variance in equation 5. The remaining term, f_0, is an estimator of the residual spectrum at frequency zero. The asymptotic distribution of the PP modified *t*-ratio is the same as that of the ADF test [30].

2.5. Statistical Software

The statistical and econometric software Eviews-9 was used for all the analytical work. It is based on the least squares optimization criterion.

2.6. Forecasting validation

The basic statistics which have been used in the evaluation of the model performance are: Mean Absolute Error (MAE), Root Mean Squared Error (RMSE) , Coefficient of Determination (R^2) , Nash-Suttcliffe Efficiency (NSE) , and Theil Inequality Coefficient (TIC).

1. Mean Absolute Error:

$$MAE = \frac{1}{n}\sum_{i=1}^{n}|Y_i - F_i| \quad (8)$$

2. Root Mean Squared Error:

$$RMSE = \sqrt{\frac{1}{n}\sum_{i=1}^{n}(Y_i - F_i)^2} \quad (9)$$

3. Coefficient of Determination:

$$R^2 = \left[\frac{\sum_{i=1}^{n}(Y_i - \bar{Y})(F_i - \bar{F})}{\sqrt{\sum_{i=1}^{n}(Y_i - \bar{Y})^2 \sum_{i=1}^{n}(F_i - \bar{F})^2}}\right]^2 \quad (10)$$

4. Nash–Sutcliffe efficiency:

$$NSE = 1 - \frac{\sum_{i=1}^{n}(Y_i - F_i)^2}{\sum_{i=1}^{n}(Y_i - \bar{Y})^2} \quad (11)$$

5. Theil Inequality Coefficient:

$$TIC = \frac{\sqrt{\frac{1}{n}\sum_{i=1}^{n}(Y_i - F_i)^2}}{\sqrt{\frac{1}{n}\sum_{i=1}^{n}(Y_i)^2} + \sqrt{\frac{1}{n}\sum_{i=1}^{n}(F_i)^2}} \quad (12)$$

Where, Y_i are the *n* observed flows, F_i are the *n* forecasted flows, $\bar{Y}$ is the average of the observed series, $\bar{F}$ is the average of the forecasted series.

The mean absolute error (MAE) has been used as a standard tool to measure model performance in hydrological and climatological research studies [32]. The root mean square error (RMSE) is another useful measure widely used in model evaluations [33]. Chai et al. [34] demonstrate that the RMSE is more suitable to represent model performance than the MAE when the error distribution is expected to be Gaussian. The coefficient of determination (R^2) shows the strength of fit between observed and forecasted data [35, 36]. It varies from 0 to 1, with higher values indicating better agreement between the model and the observations. The coefficient of efficiency (NSE) introduced by Nash and Sutcliffe has been widely used to evaluate the performance of hydrologic models [37, 38]. In fact, NSE is the ratio of the mean square error, to the variance in the observed data, subtracted from unity [39]. The range of NSE lies between 1 and $-\infty$. An efficiency of 1 (NSE=1) means a perfect match of model results and observed data. Theil Inequality Coefficient (TIC) is another statistical measure of forecast accuracy [40]. The range of TIC lies between 0 and 1. In practice, values of 0.55 or less are very good [41]. If the coefficient equal zero, it can be said that there is a perfect fit between the observed and the forecasted data.

3. Results and Discussion

3.1. Identification of the Model

The graphical presentation of the monthly streamflow in Figure 2 shows that there is a seasonal pattern in the series and the series is non-stationary. Most of the hydrological time series are non-stationary time series. Mohamed et al. [20, 42] observed that monthly flow time series in most of Sudanese gauging station as non-stationary time series.

The diagram of sample autocorrelation function (ACF) and partial autocorrelation function (PACF) proves that the series is non-stationary, Figure 4. Both the Phillips-Perron (PP) test and the Augmented Dickey-Fuller (ADF) test confirmed the non-stationarity of the monthly data, as shown in Table 1.

From Figure 4, it has been remarked that the data is seasonal of period 12 months and must therefore be differenced by one seasonal degree of differencing to attain

stationary (D=1). The PP and ADF tests were done again on the seasonally differenced data. The results of the tests adjudge that the differenced series is stationary, Table 2. As the time series became stationary, no non-seasonal differencing was used (d=0).

Figure 5 shows the ACF and PACF plots of the data after the taken of the seasonal difference. It emerges that most of the seasonality is vanished and the data became stable. The autocorrelation structure in Figure 5 proposes many models. The proposed models, the Akaike Information Criterion (AIC), the Hannan-Quinn Criterion (HQ) and the coefficient of determination (R^2) values are shown in Table 3. The model that gives the minimum value of AIC and HQ with a maximum value of R^2 is selected as best model.

Clearly, model SARIMA $(1,0,1)\times(0,1,1)_{12}$ has the smallest values of AIC, HQ and the maximum value of R^2 then one would provisionally have a model SARIMA $(1,0,1)\times(0,1,1)_{12}$.

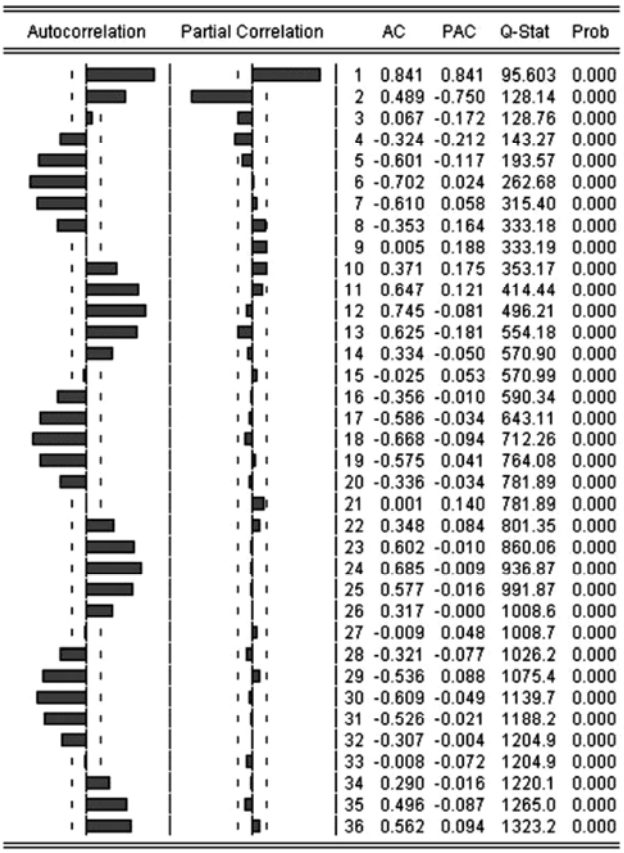

Autocorrelation	Partial Correlation		AC	PAC	Q-Stat	Prob
		1	0.841	0.841	95.603	0.000
		2	0.489	-0.750	128.14	0.000
		3	0.067	-0.172	128.76	0.000
		4	-0.324	-0.212	143.27	0.000
		5	-0.601	-0.117	193.57	0.000
		6	-0.702	0.024	262.68	0.000
		7	-0.610	0.058	315.40	0.000
		8	-0.353	0.164	333.18	0.000
		9	0.005	0.188	333.19	0.000
		10	0.371	0.175	353.17	0.000
		11	0.647	0.121	414.44	0.000
		12	0.745	-0.081	496.21	0.000
		13	0.625	-0.181	554.18	0.000
		14	0.334	-0.050	570.90	0.000
		15	-0.025	0.053	570.99	0.000
		16	-0.356	-0.010	590.34	0.000
		17	-0.586	-0.034	643.11	0.000
		18	-0.668	-0.094	712.26	0.000
		19	-0.575	0.041	764.08	0.000
		20	-0.336	-0.034	781.89	0.000
		21	0.001	0.140	781.89	0.000
		22	0.348	0.084	801.35	0.000
		23	0.602	-0.010	860.06	0.000
		24	0.685	-0.009	936.87	0.000
		25	0.577	-0.016	991.87	0.000
		26	0.317	-0.000	1008.6	0.000
		27	-0.009	0.048	1008.7	0.000
		28	-0.321	-0.077	1026.2	0.000
		29	-0.536	0.088	1075.4	0.000
		30	-0.609	-0.049	1139.7	0.000
		31	-0.526	-0.021	1188.2	0.000
		32	-0.307	-0.004	1204.9	0.000
		33	-0.008	-0.072	1204.9	0.000
		34	0.290	-0.016	1220.1	0.000
		35	0.496	-0.087	1265.0	0.000
		36	0.562	0.094	1323.2	0.000

Figure 4. *ACF and PACF plots for White Nile River monthly flow.*

Table 1. *Unit root test of the monthly flow data.*

Test	Static	P-value
Augmented Dickey-Fuller	0.056	0.699
Phillips-Perron	-1.137	0.232

Table 2. *Unit root test of the differenced data.*

Test	Static	P-value
Augmented Dickey-Fuller	-3.725	0.000
Phillips-Perron	-3.678	0.000

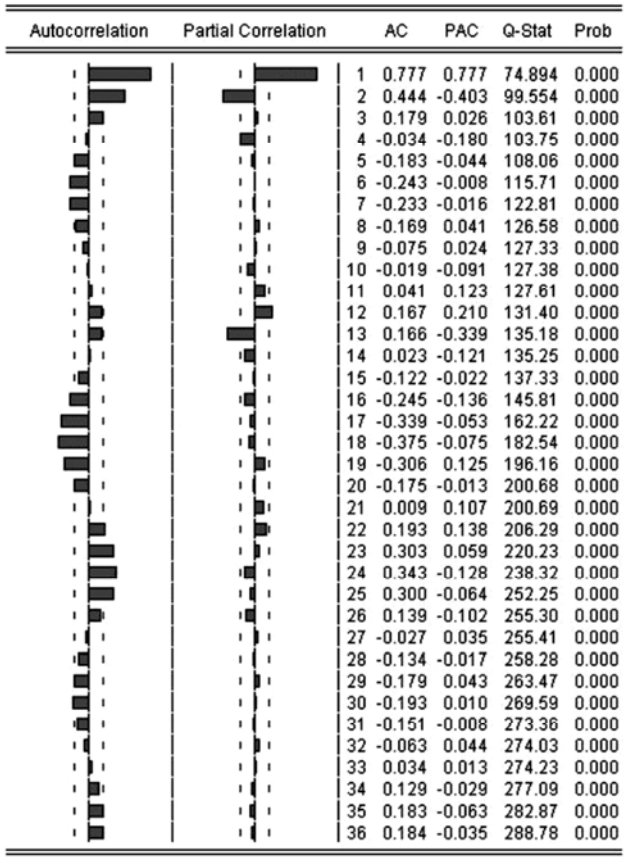

Autocorrelation	Partial Correlation		AC	PAC	Q-Stat	Prob
		1	0.777	0.777	74.894	0.000
		2	0.444	-0.403	99.554	0.000
		3	0.179	0.026	103.61	0.000
		4	-0.034	-0.180	103.75	0.000
		5	-0.183	-0.044	108.06	0.000
		6	-0.243	-0.008	115.71	0.000
		7	-0.233	-0.016	122.81	0.000
		8	-0.169	0.041	126.58	0.000
		9	-0.075	0.024	127.33	0.000
		10	-0.019	-0.091	127.38	0.000
		11	0.041	0.123	127.61	0.000
		12	0.167	0.210	131.40	0.000
		13	0.166	-0.339	135.18	0.000
		14	0.023	-0.121	135.25	0.000
		15	-0.122	-0.022	137.33	0.000
		16	-0.245	-0.136	145.81	0.000
		17	-0.339	-0.053	162.22	0.000
		18	-0.375	-0.075	182.54	0.000
		19	-0.306	0.125	196.16	0.000
		20	-0.175	-0.013	200.68	0.000
		21	0.009	0.107	200.69	0.000
		22	0.193	0.138	206.29	0.000
		23	0.303	0.059	220.23	0.000
		24	0.343	-0.128	238.32	0.000
		25	0.300	-0.064	252.25	0.000
		26	0.139	-0.102	255.30	0.000
		27	-0.027	0.035	255.41	0.000
		28	-0.134	-0.017	258.28	0.000
		29	-0.179	0.043	263.47	0.000
		30	-0.193	0.010	269.59	0.000
		31	-0.151	-0.008	273.36	0.000
		32	-0.063	0.044	274.03	0.000
		33	0.034	0.013	274.23	0.000
		34	0.129	-0.029	277.09	0.000
		35	0.183	-0.063	282.87	0.000
		36	0.184	-0.035	288.78	0.000

Figure 5. *ACF and PACF plots after one seasonal difference.*

3.2. Estimation of the Parameter

The second part of the Box-Jenkins methodology for SARIMA modeling is the parameter estimation. After the selection of the best model using the AIC, HQ and R^2 criteria, estimation of the parameters was conducted. The value of the parameters, associated standard errors, t-statistic and p-values are accessible in Table 4. The results confirmed that the parameters are significant as their p-value < 0.050. All the absolute values of the inverted AR and MA roots are smaller than one; consequently the model is stationary and invertible.

3.3. Diagnostic Check

Once the suitable model is selected, the Box-Jenkins methodology requires examining the residuals of the model to prove that the model is adequate one for the time series. The residuals should behave like Gaussian white noise, which is appearing random, homoscedastic and normal [24]. Different verification tests were applied on the residual series. These tests are discussed briefly in the next paragraphs.

3.3.1. ACF and PACF of Residuals

The residuals autocorrelation function (RACF) and residuals partial autocorrelation function (RPACF) are useful tools to assess the presence of correlation between the residuals. The RACF and RPACF of the model SARIMA $(1,0,1)\times(0,1,1)_{12}$ are shown in Figure 6. All values of the RACF and RPACF lie within the confidence limits. The figure noticeably supports the absence of significant

correlation between the residuals.

Table 3. *Comparison of the proposed Model (Malakal Station).*

Variable	Model	AIC	HQ	R^2
Mean Monthly Flow	SARIMA $(1,0,1)\times(0,1,1)_{12}$	6.2053	6.2432	0.828
	SARIMA $(1,0,0)\times(0,1,1)_{12}$	6.3013	6.3203	0.805
	SARIMA $(1,0,1)\times(1,1,1)_{12}$	6.5413	6.6021	0.787
	SARIMA $(1,0,1)\times(1,1,0)_{12}$	6.5647	6.6052	0.774

Table 4. *Estimation of the SARIMA $(1,0,1)\times(0,1,1)_{12}$ model.*

Variable	Coefficient	Std. Error	t-Statistic	Prob.
AR (1)	0.705310	0.076140	9.263267	0.0000
MA (1)	0.457969	0.095059	4.817725	0.0000
MA (12)	-0.877046	0.040991	-21.39617	0.0000
MA (13)	- 0.418906	0.088002	-4.760182	0.0000
R-squared	0.828983	Mean dependant var		-0.5021
Adjusted R-squared	0.824521	S. D. dependant var		12.645
S. E. of regression	5.297306	Akaike info criterion		6.2053
Sum squared resid.	3227.067	Schwarz criterion		6.2987
Log likelihood	-365.2159	Hannan-Quinn criterion		6.2432
Durbin-Watson stat	2.005604			
Inverted AR roots	0.71			
Inverted MA roots	0.99	.86+.49 i	.86 -.49 i	.50-.86 i
	.50+.86 i	.00-.99 i	.00+.99 i	-0.48
	-.49+.86 i	-.49-.86 i	-.85+.50 i	-.85-.50 i
	-0.99			

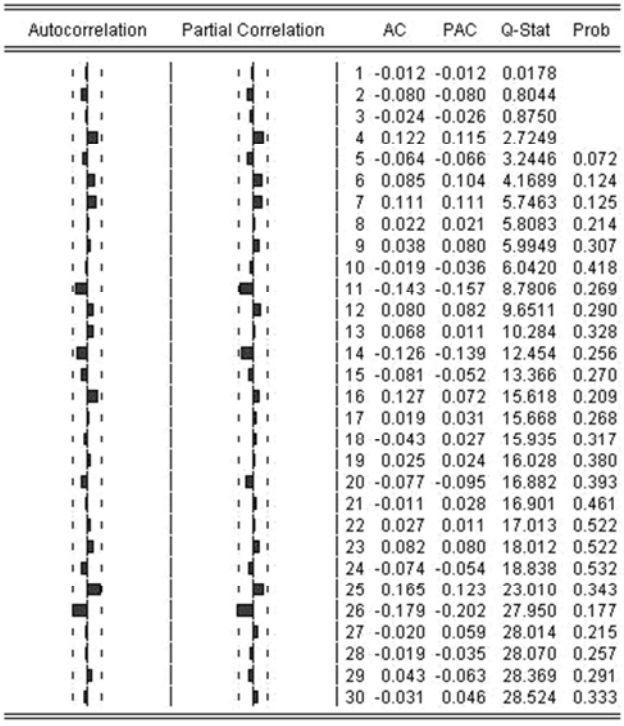

Figure 6. *RACF and RPACF plots for SARIMA $(1,0,1)\times(0,1,1)_{12}$.*

3.3.2. The Ljung-Box Test

The Ljung-Box test is used for checking independence (randomness) of residual. From Figure 6, the goodness of fit values for the autocorrelations of residuals from the model up to lag 30 was greater than 0.050. The result proves the acceptance of the null hypothesis of model adequacy at the 5% significance level and the set of autocorrelations of residuals was considered white noise.

3.3.3. The Durbin-Watson Statistic

The Durbin-Watson (DW) statistic measures the serial correlation in the residuals. If the residuals are not correlated, the Durbin-Watson statistic will be 2 [43, 44]. The Durbin-Watson test statistic value in Table 4 is found to be 2.0056, which does not deviate from 2 by more than 0.0056. Hence, there is no serial correlation between the residuals.

3.3.4. The Breusch-Godfrey Test

The Breusch-Godfrey test is an alternative to the Durbin-Watson test [45]. The test belongs to the class of asymptotic (large sample) tests known as Lagrange multiplier (LM) tests. The Serial Correlation LM test in Table 5 has the *p*-value > 0.050. Therefore, it accepts the hypothesis of no serial correlation in the residuals.

Table 5. *The Breusch-Godfrey serial correlation LM test.*

F-statistic	2.216	Prob. F (2,113)	0.114
Obs*R-squared	4.079	Prob. Chi-square (2)	0.130

F-statistic	1.06	Prob. F (12,103)	0.401
Obs*R-squared	12.704	Prob. Chi-square (2)	0.391

3.3.5. Runs Test for Serial Correlation

Another approach to testing for serial correlation in the residuals is to use the runs test [46]. The runs test, or Wald–Wolfowitz test, is a simple non-parametric test for randomness. The high *p*-value of the runs test [0.795] confirms that there is no serial correlation between the residuals.

3.3.6. Normality Tests

The Kolmogorov-Smirnov (K-S) test is a non-parametric test of data fitting to a theoretical distribution

using the maximum deviation (D_{max}) between the two functions of cumulative distribution [47]. The value of the maximum deviation D_{max} is compared with the critical value D_{crt}. If the maximum deviation is greater than the critical value the assumption of normality is rejected. The test is used to examine the normality of the residuals series. It is observed that the maximum deviation D_{max} is less than the critical value D_{crt} at 5% significance level as shown in Table 6. The test shows that the residuals are normally distributed since the *p*-value > 0.050 [*p*-value=0.195]. In addition to Kolmogorov-Smirnov test, the histogram of the residuals, Figure 7, shows that the data distribution is fairly normal.

3.3.7. Homoscedasticity Tests

Homoscedasticity is the term used to define that the variance of the residual in each observation is constant. For the diagnostic checking of residuals in terms of homoscedasticity, Breusch-Pagan-Godfrey, Harvey, Glejser, and ARCH LM tests are commonly used for time series data. In this research, ARCH LM test, which is a Lagrange multiplier (LM) test, is used for autoregressive conditional heteroscedasticity (ARCH) in the residuals [48]. Test statistics value of ARCH test for the homoscedasticity of the residuals is presented in Table 7. The *p*-value > 0.050, this indicates that the residual variance is constant. Lastly, the selected SARIMA $(1,0,1)\times(0,1,1)_{12}$ model seems to be very closely aligned with the actual data as shown in Figure 8.

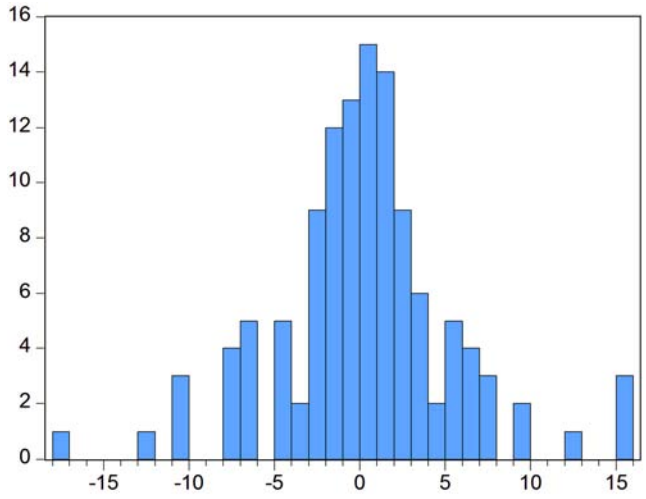

Figure 7. *Histogram of the Residuals.*

Table 6. *K-S Test Calculation for Residuals.*

One-Sample Kolmogorov-Smirnov Test	
Maximum deviation (D_{max})	0.099
Critical value (D_{crt})	0.125

Table 7. *ARCH LM test.*

F-statistic	0.171	Prop. F (2,114)	0.843
Obs*R-squared	0.349	Prop. Chi-square (2)	0.840

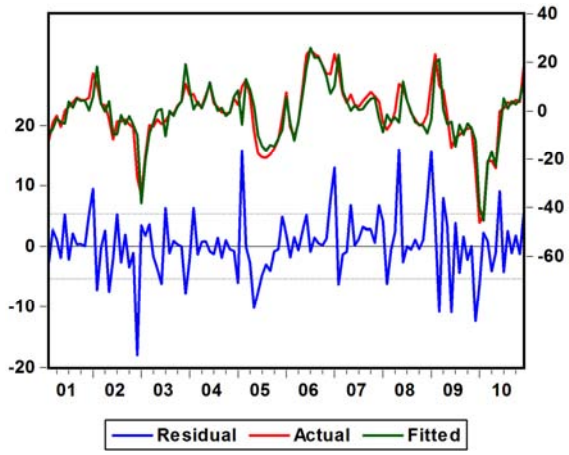

Figure 8. *Comparison of actual data and SARIMA model [2000–2010].*

Table 8. *Forecasting accuracy statistics.*

Statistic measures	Value
RMSE	8.660
MAE	5.473
R^2	0.869
NSE	0.853
TIC	0.048

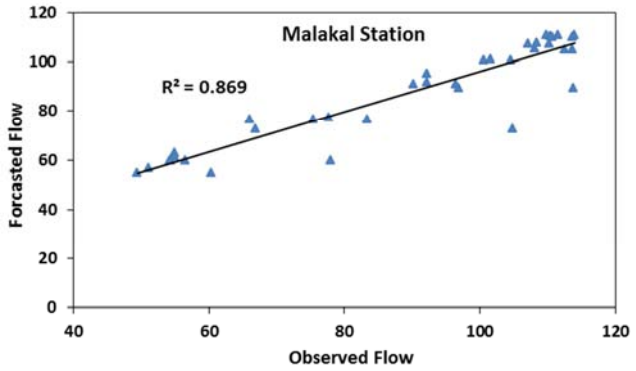

Figure 9. *Calibration results of SARIMA $(1,0,1)\times(0,1,1)_{12}$ model.*

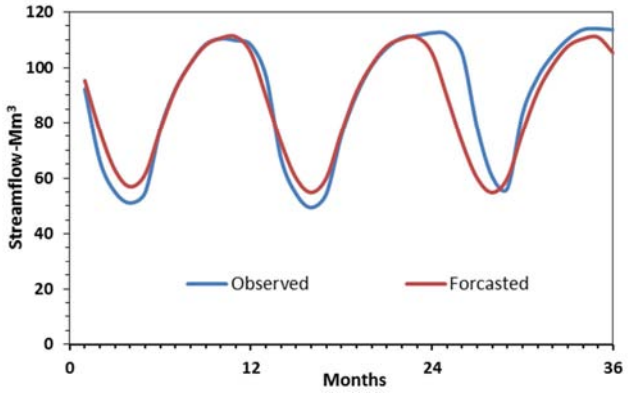

Figure 10. *Forecasting of monthly streamflow using SARIMA $(1,0,1)\times(0,1,1)_{12}$ model, [2011–2013].*

3.4. Forecasting of Monthly Flow

The selected model was tested for its validity to forecast 36 observations obtained for the years 2011 to 2013 for the White Nile River.

If the selected model has to perform well in forecasting phase, the forecast error will be very small. The accuracy of forecasts was examined using the root mean square error (RMSE), the mean absolute error (MAE), the coefficient of determination (R^2), Nash-Sutcliffe efficiency criteria (NSE) and Theil inequality coefficient (TIC). Table 8 shows the statistic measures. It is observed that the model has lower values of MAE and RMSE. The coefficient of determination value of 0.869, Figure 9, and Nash-Sutcliffe efficiency criteria (NSE) value of 85.3% showed the very good performance of the model. Theil inequality coefficient turns out to be 0.048, which indicates a perfect fit. The observed flow was found to be closely aligned to the forecasted values as shown in Figure 10. Eventually, this proves that the SARIMA $(1,0,1)\times(0,1,1)_{12}$ model identified previously is sufficient.

3.5. Discussion

SARIMA models have been used to monthly flow of White Nile River. The AIC and HQ criterion suggest that a SARIMA $(1,0,1)\times(0,1,1)_{12}$ should be fit for the monthly flow. Based on the Box-Jenkins methodology, the residuals should behave like Gaussian white noise which is appearing random, homoscedastic and normal process. Randomness analysis of the residuals was tested by the Ljung-Box, Durbin-Watson Statistic, Breusch-Godfrey, and runs tests. The homoscedasticity of residuals was examined by the ARCH LM test. To prove whether the residuals are normally distributed, Kolmogorov-Smirnov test was applied. The selected SARIMA model has fulfilled all the above tests.

Further, five measures for judging forecast accuracy of the selected model have been used. In practice, it is better to use more than one performance criteria. This will assist to obtain a good information about the amount and magnitude of the overall forecast error. The model has passed all tests, and the results reveal the ability of SARIMA to provide accurate forecast. Finally, the appropriate selection of the model orders is extremely important for successful forecasting.

4. Conclusion

Monthly flow forecasting is an important component in planning and management of water resources in Sudan. For example, the operation of Jabal al Awliya dam in the White Nile River is completely depending on the measured flow at Malakal station. This paper applied the seasonal autoregressive integrated moving average (SARIMA) models in forecasting monthly flow at the Malakal station on the White Nile River, South Sudan.

The best model that fits the criteria and meets the requirements is SARIMA $(1,0,1)\times(0,1,1)_{12}$. The model was applied to forecast three years monthly flow values. By analyzing the forecasted values, it was found that use of SARIMA model for forecasting streamflow is marvelously good. Consequently, the developed model will help water resources directors for management of the White Nile, and optimal operation of Jabal al Awliya dam. Water resources experts and decision makers are expected to find this model useful in the design of water policies in both country Sudan and South Sudan.

Nomenclature

ACF	Autocorrelation Function
ADF	Augmented Dickey Fuller
AIC	Akaike Information Criterion
ARIMA	Autoregressive Integrated Moving Average
ARMA	Autoregressive and Moving Average
ARCH	Autoregressive Conditional Heteroscedasticity
AR (p)	Autoregressive parameter of order (p)
DF	Dickey Fuller
DW	Durbin-Watson
HQ	Hannan-Quinn Criterion
K-S	Kolmogorov-Smirnov
LM	Lagrange multiplier test
MAE	Mean Absolute Error
MA (q)	Moving average parameter of order (q)
NBI	Nile Basin Initiative
NSE	Nash–Sutcliffe efficiency
PACF	Partial Autocorrelation Function
PP	Phillips-Perron test
RACF	Residuals Autocorrelation Function
RPACF	Residuals Partial Autocorrelation Function
RMSE	Root Mean Squared Error
R^2	Coefficient of determination
SARIMA	Seasonal Autoregressive Integrated Moving Average
TIC	Theil Inequality Coefficient

References

[1] The Nile Basin Initiative (NBI) (2016) Annual Report. [E-book] Available: www.nilebasin.org.

[2] Melesse A (2011) Nile River Basin: Hydrology, Climate and Water Use. Springer Dordrecht Heidelberg, New York.

[3] Sutcliffe JV, Parks YP (1987) Hydrological modeling of the Sudd and Jonglei Canal. Hydrolog Sci J, 32: 2: 143-159.

[4] Ardiclioglu M, Kuriqi A (2019) Calibration of channel roughness in intermittent rivers using HEC-RAS model: case of Sarimsakli creek, Turkey. SN Appl. Sci. 1, 1080. https://doi.org/10.1007/s42452-019-1141-9.

[5] Liu T, Chen Y, Li B, Hu Y, Qiu H, Liang Z (2019) Long-term streamflow forecasting for the Cascade Reservoir System of Han River using SWAT with CFS output. Hydrology Research, 50 (2): 655–671. https://doi.org/10.2166/nh.2018.114.

[6] Wang W (2006) Stochasticity, Nonlinearity and Forecasting of Streamflow Processes. IOS Press, Amsterdam.

[7] Makkeasorn A, Chang N, Zhou X (2008) Short-Term Streamflow Forecasting With Global Climate Change Implications– A Comparative Study Between Genetic Programming and Neural Network Models. J HYDROL. 352: 336-354. https://doi.org/10.1016/j.jhydrol.2008.01.023.

[8] Teng J, Chiew FHS, Vaze J, Post D (2011) Calibration of hydrological models for medium-term streamflow prediction in a changing climate. IAHS-AISH Publication. 344: 221-226.

[9] Li X, Sha J, Wang ZL (2019) Comparison of daily streamflow forecasts using extreme learning machines and the random forest method, Hydrological Sciences Journal, 64: 15, 1857-1866. DOI: 10.1080/02626667.2019.1680846.

[10] Sharma S, Siddique R, Reed S, Ahnert P, Mejia A (2019) Hydrological Model Diversity Enhances Streamflow Forecast Skill at Short- to Medium-Range Timescales. Water Resour. Res., 55 (2): 1510-1530. https://doi.org/10.1029/2018WR023197.

[11] Wu J, Liu H, Wei G, Song T, Zhang C, Zhou H. (2019) Flash Flood Forecasting Using Support Vector Regression Model in a Small Mountainous Catchment. Water. 11. 1327. 10.3390/w11071327.

[12] Nacar S, Hınıs MA, Kankal M (2018) Forecasting Daily Streamflow Discharges Using Various Neural Network Models and Training Algorithms. KSCE J Civ Eng 22, 3676–3685. https://doi.org/10.1007/s12205-017-1933-7.

[13] Bai Y, Bezak N, Sapač K, Klun M, Zhang J (2019) Short-Term Streamflow Forecasting Using the Feature-Enhanced Regression Model. Water Resour Manag. 33: 4783–4797. https://doi.org/10.1007/s11269-019-02399-1.

[14] Hipel KW, McLeod A I (1994) Time Series Modelling of Water Resources and Environmental System, Elsevier, Amsterdam.

[15] Abrahart R, See L (2000) Comparing neural network and autoregressive moving average techniques for the provision of continuous river flow forecasts in two contrasting catchments. Hydrol Process 14: 2157-2172.

[16] De silva MAP (2006) A time series model to predict the runoff ratio of catchment of the Kalu ganga basin, J. Natn. Sci. Foundation Sri Lanka, 34 (2): 103-105. DOI: 10.4038/jnsfsr.v34i2.2089.

[17] Modarres R (2007) Streamflow drought time series forecasting. Stochastic Environ. Res. Ris Assess 21: 223-233. https://doi.org/10.1007/s00477-006-0058-1.

[18] Rabenja AT, Ratiarison A, Rabeharisoa JM (2009) Forecasting of the rainfall and the discharge of the Namorona River in Vohiparara and FFT analyses of these data, Proceedings, 4th International conference in High-Energy Physics, Antananarivo, Madagascar, 1–12.

[19] Valipour M (2015) Long-term runoff study using SARIMA and ARIMA models in the United States. Meteorol Appl 22 (3): 592-598.

[20] Mohamed TM, Etuk EH (2017) Application of linear stochastic models to monthly streamflow data of Rahad River, Sudan. IJHST, 7 (2): 197-212. https://doi.org/10.1504/IJHST.2017.084144.

[21] Fashae OA, Olusola AO, Ndubuisi I, Udomboso C G (2019) Comparing ANN and ARIMA model in predicting the discharge of River Opeki from 2010 to 2020, River Research and Applications, 2: 169-177. https://doi.org/10.1002/rra.3391.

[22] Le Houérou HN (2009) Bioclimatology and Biography of Africa, Verlag Berlin Heidelberg, Germany.

[23] Sutcliffe JV, Parks YP (1999) The Hydrology of the Nile, IAHS Special Publication no. 5, IAHS Press, Institute of Hydrology, Wallingford, UK.

[24] Box GEP, Jenkins GM, Reissel GC, Ljung GM (2015) Time Series Analysis Forecasting and Control. 5th edition, Prentice Hall, USA. ISBN: 978-1-118-67491-8.

[25] Akaike H (1974) A New look at the statistical model identification. IEEE Trans. Autom. Control 19 (6): 716–723.

[26] Hannan EJ, Quinn BG (1979) The determination of the order of an autoregression, J R STAT SOC B, (41), 190-195.

[27] Mainassara YB, Kokonendji CC (2015) Modified Schwarz and Hannan–Quinn information criteria for weak VARMA models. Stat Inference Stoch Process, 19: 199–217. https://doi.org/10.1007/s11203-015-9123-z.

[28] Kwiatkowski D, Phillips P, Schmidt P, Shin, Y (1992) Testing the null hypothesis of stationarity against the alternative of a unit root. J. Econom., 54 (1-3): 159-178.

[29] Zivot E, Andrews D (1992) Further evidence on the great crash, the oil-price shock, and the unit-root hypothesis. J Bus Econ Stat, 10 (3): 251-270. www.jstor.org/stable/1391541.

[30] EViews 9 User's Guide II (2015) IHS Global Inc. Web: www.eviews.com.

[31] Phillips P, Perron P (1988) Testing for a Unit Root in Time Series Regression. Biometrika: 75: 335–346.

[32] Willmott C J, Matsuura K (2005) Advantages of the mean absolute error (MAE) over the root mean square error (RMSE) in assessing average model performance, Clim. Res. 30: 79–82.

[33] Dubey AK, Chembolu V, Gupta PK, Dutta S, Singh RP (2019) Application of Satellite Altimetry in Understanding River-Wetland Flow Interactions of Kosi River. J Earth Syst Sci 128, 89. https://doi.org/10.1007/s12040-019-1099-4.

[34] Chai T, Draxler R (2014) Root mean square error (RMSE) or mean absolute error (MAE)? – Arguments against avoiding RMSE in the literature. Geosci. Model Dev. 7: 1247–1250.

[35] Singh P, Kumar A, Kumar N, Kishore Naval. (2010). Hydro-meteorological correlations and relationships for estimating streamflow for Gangotri Glacier basin in Western Himalayas. International Journal of Water Resources and Environmental Engineering. 2. 60-69.

[36] Yang Q, Wang Y, Zhang J. et al. A (2017) comparative study of shallow groundwater level simulation with three time series models in a coastal aquifer of South China. Appl Water Sci 7: 689–698. https://doi.org/10.1007/s13201-015-0282-2.

[37] Nash JE, Sutcliffe JV (1970) River flow forecasting through conceptual models: A discussion of principles, J HYDROL, 10 (3): 282–290.

[38] Kumar A, Sharma MP (2016) A modeling approach to assess the greenhouse gas risk in Koteshwar hydropower reservoir. India, Hum Ecol Risk Assess, 22 (8): 1651-1664. DOI: 10.1080/10807039.2016.1209077.

[39] David R, Legates DR, McCabe GJ (1999) Evaluating the use of "goodness-of-fit" measures in hydrologic and hydroclimatic model validation. Water Resour. Res., 35 (1): 233-241.

[40] Yorucu V (2003) The Analysis of Forecasting Performance by Using Time Series Data for Two Mediterranean Islands. Rev. Soc. Econ. Bus. Stud., 2: 175-196.

[41] Lindberg B (1982) International Comparison of Growth in Demand for a New Durable Consumer Product, J Mark Res., 19, 364-371.

[42] Mohamed TM, Etuk EH (2016) Simulation of Monthly Flow for the Dinder River, Sudan. Journal of Basic and Applied Research International 14 (4): 265-271.

[43] Montgomery DC, Peck EA, Vining GG (2006) Introduction to Linear Regression Analysis. 4th Edition, John Wiley & Sons, UK.

[44] Kleinbaum DG, Kupper LL, Nizam A, Muller KE (2007) Applied Regression Analysis and Multivariable Methods. 4th Edition, Duxbury Press, Pacific Grove, USA.

[45] Diebold FX (2016) Econometrics, Department of Economics, University of Pennsylvania. http://www.ssc.upenn.edu/~fdiebold/Textbooks.html.

[46] Draper ND, Smith ND (1981) Applied Regression Analysis, Wiley & Sons, New York, second edition.

[47] Yüreki K, Kurunc A, Ozturk F (2005) Testing the Residuals of an ARIMA Model on the Cekerek Stream Watershed in Turkey. Turkish J Eng Env Sci. 29: 61-74.

[48] Engle RF (1982) Autoregressive Conditional Heteroscedasticity with Estimates of the Variance of United Kingdom Inflation. Econometrica, 50: 987–1008.